Materials Research, Vol. 8, No. 2, 201-205, 2005

Dilatometric Studies of (SiO_2-RE_2O_3-Al_2O_3) Silicon Carbide Ceramics

Juliana Marchi*, José Carlos Bressiani, Ana Helena de Almeida Bressiani

Instituto de Pesquisas Energéticas e Nucleares, IPEN
Av. Prof. Lineu Prestes, 2242, 05508-000 Cidade Universitária, São Paulo - SP, Brazil

Received: November 23, 2003; Revised: March 13, 2005

Silicon carbide is an important structural ceramic and finds applications as abrasives, as a refractory and in automotive engine components. This material can attain high densities during liquid phase sintering if suitable additives are used. Silicon carbides containing silica, alumina and rare earth oxides have suitable characteristics to promote liquid phase sintering. In this paper, the sintering behavior of silicon carbide ceramics with additives based on the (SiO_2-RE_2O_3-Al_2O_3) system (RE = Y, Dy) has been studied. Samples with different compositions and containing 90 vol.% SiC were sintered in a dilatometer at 1950 °C/1h and in a graphite resistance furnace from 1500 °C/1h up to 1950 °C/1h. The shrinkage behavior as a function of rare earth oxide used and additive composition was also studied. The sintered materials were characterized by density and weight loss measurements. The crystalline phases were identified by X-ray diffraction analysis. The sintering kinetics of these materials can be related to the formation of secondary crystalline phases.

Keywords*: sintering, silicon carbide, oxide additives*

1. Introduction

Silicon carbide is one of the most important structural ceramic material with high temperature strength, low density, and excellent wear as well as thermal shock resistance. Due to this unique combination of properties, these materials can be used in a large number of applications, such as automotive heat engines, cutting tools, heat exchangers and as mechanical seals.

Sintering of silicon carbide can be done through solid state mechanisms[1,2] or in the presence of a liquid phase[1-9], through a dissolution re-precipitation process. In the first one, carbon is the main additive, usually in combination with boron or aluminium. If oxide additives are used, sintering of silicon carbide occurs through liquid phase, which is generally produced by a reaction between the additives and the SiO_2 present on the SiC surface[10]. The main advantage of this approach is that lower temperatures are involved and the microstructure is more homogeneous.

Silicon carbide can reveal several polymorphs[11-12], in which the basic tetrahedron (Figure 1) is formed with one silicon atom and four carbon atoms (or vice versa). These tetrahedrons are linked at their corners. The difference in the polymorphs is the sequential stacking of planar layers of closed-packed atoms. The 3C polymorph has a cubic unit cell, with (ABCABC…) sequence layers, and is known as β-silicon carbide. The other polymorphs are called α-silicon carbide.

The composition of the liquid is an important parameter in liquid phase sintering of silicon carbide. This phase must have adequate viscosity to make material transport more efficient, and consequently improve densification[13-16].

Sintering additives based on the SiO_2-Al_2O_3-RE_2O_3 system (RE = rare earth element) have been found to be effective to obtain high density silicon carbide ceramics [17-19], as well as silicon nitride ceramics[20-22], through liquid phase sintering. The liquid phase dissolves the silicon carbide particles at relatively low temperatures.

The sintering behavior of silicon carbide with (SiO_2-Al_2O_3-Y_2O_3) additives was presented elsewhere and the sintering kinetics was not fully understood[23]. In this paper, the sintering kinetics of silicon carbide ceramics has been studied with the help of additives based on the (SiO_2-RE_2O_3-Al_2O_3) system (RE = Y, Dy). The sintering behavior can be related to the formation of secondary crystalline phases.

2. Experimental Procedure

RE_2O_3 (RE = Y and Dy from H. C. Stark), SiO_2 (Sigma Aldrich) and Al_2O_3 (A16, Alcoa) were used as additives to the silicon carbide ceramics. Specimens with four different compositions containing 10 vol. % of additives (Table 1) and 90 vol. % of β-SiC (BF 17, H. C. Stark) were studied to evaluate the effect of composition and rare earth elements on densification of silicon carbide based materials. The theoretical densities of the final mixtures were calculated using the rule of mixtures (Table 1).

The silicon carbide and additives were mixed, milled in an attritor for 4 hours and dried in an evaporator (Heidolph WB 2000). The powder mixtures were uniaxially and cold isostatically pressed. The green densities of the compacts were determined.

Sintering studies were performed in a dilatometer (Netzsch, DIL, 402 E/7) with 15 °C/min heating rate up to 1950 °C/1h, in flowing argon (1 atm) and in a furnace with graphite heating elements, wherein a protective powder bed with RE 60 composition was used. The heating schedule used in the dilatometer experiments was used in the experiments carried out with the furnace with several dwell temperature: 1500 °C/1h; 1600 °C/1h; 1700 °C/1h; 1800 °C/1h; 1950 °C/1h.

The final density (Archimedes method) and weight loss during sintering were evaluated. The crystalline phases in the samples after each heat treatment were determined from X-ray diffraction measurements. (Phillips, PW, 1710) The microstructures were examined in a scanning electron microscope (Philips, XL, 30) using longitudinal sections of plasma etched samples prepared using conventional methods.

Table 1. Composition characteristics.

composition	Mol (%)				Theoretical Density (g/cm^3)	Weight (%)	
	SiO_2	Al_2O_3	Y_2O_3	Dy_2O_3		SiC	additive
Y 33	33.33	33.33	33.33	-	3.2954	87.39	12.61
Dy 33	33.33	33.33	-	33.33	3.4370	83.79	16.21
Y 60	60	20	20	-	3.2463	88.68	11.32
Dy 60	60	20	-	20	3.3434	86.14	13.86

---

*e-mail: jmarchi@ipen.br

3. Results and Discussion

3.1. Density

The densification results of samples RE60 and RE33, sintered at 1950 °C/1h in the furnace with graphite heating elements are shown in Table 2. The density data show that samples sintered with yttria exhibit higher densities and weight losses compared to samples sintered with dysprosia. Further, the RE33 samples have higher densities with lower weight losses compared to the RE60 samples.

3.2. Microstructural observations

The X-ray diffraction results indicate that α (4H, 6H and 15R) and β (3C) silicon carbide polymorphs were present in all samples, independent of the composition or the sintering temperature as they were primarily crystalline phases. Presence of the 3C polymorph indicates that the β-α transformation is incomplete.

In the RE33 samples sintered with yttria, depending on the heat treatment temperature, $Y_4Al_2O_9$, YAG, $Y_{4,67}(SiO_4)_3O$, $Y_2Si_2O_7$ and $Y_2Al_2O_6$ (YAP) were identified by X-ray diffraction as crystalline secondary phases. In samples sintered with dysprosia, DyAG and $Dy_2Al_2O_6$ (DyAP) were identified as the crystalline secondary phases. Table 3 shows the crystalline secondary phases at each heat treatment temperature, with both the rare earth oxides.

The X-ray diffraction patterns of bulk RE33 samples, heat treated at 1800 °C/1h, are shown in Figure 2.

The X-ray diffraction results of RE60 samples sintered at temperatures up to 1600 °C, reveal no secondary crystalline phases. In the dysprosia containing sample sintered at 1700 °C, DyAP was identified as the secondary crystalline phase. At this temperature, in the sample containing yttria no secondary crystalline phases were identified. At higher temperatures, several RE based secondary crystalline phases were identified (Table 3).

The X-ray diffraction patterns of bulk RE60 samples heat treated at 1800 °C/1h, are shown in Figure 3.

The secondary phase appears to be well distributed in almost all samples, indicating good homogeneity in the mixture (Figure 4). An exception to this can be observed in the Dy33 sample (Figure 4b) which shows more secondary phase. This explains the lower density of this sample. The morphology of silicon carbide grains could be revealed by plasma etching, and normal distribution was observed in all the sintered samples. No secondary or abnormal grain growth was observed.

Table 2. Densification results after sintering in graphite resistance furnace.

composi-tion	Samples sintered with yttria		Samples sintered with disprosia	
	Density (%td)	Weight loss (%)	Density (%td)	Weight loss (%)
RE60	90.37 ± 0.71	7.76 ± 0.05	82.22 ± 0.99	7.29 ± 0.14
RE33	95.43 ± 0.32	6.45 ± 0.15	90.49 ± 0.26	5.20 ± 0.25

Table 3. Crystalline secondary phases in RE sintered samples, according to each thermal treatment temperature.

Temperature of thermal treatment	RE 33 samples		RE 60 samples	
	RE = Y	RE = Dy	RE = Y	RE = Dy
1500°/1h	$Y_4Al_2O_9$; YAG $Y_{4,67}(SiO_4)_3O$	DyAG	-	-
1600°/1h	$Y_{4,67}(SiO_4)_3O$	DyAG	-	-
1700°/1h	$Y_2Si_2O_7$	-	-	$Dy_2Al_2O_6$
1800°/1h	$Y_2Al_2O_6$	$Dy_2Al_2O_6$	YAG	$Dy_2Al_2O_6$
1950°/1h	$Y_2Al_2O_6$ $Y_4Al_2O_9$	$Dy_4Al_2O_9$	$Y_4Al_2O_9$ $Si_2Al_6O_{13}$	$Dy_4Al_2O_9$ $Dy_2Al_vO_6$

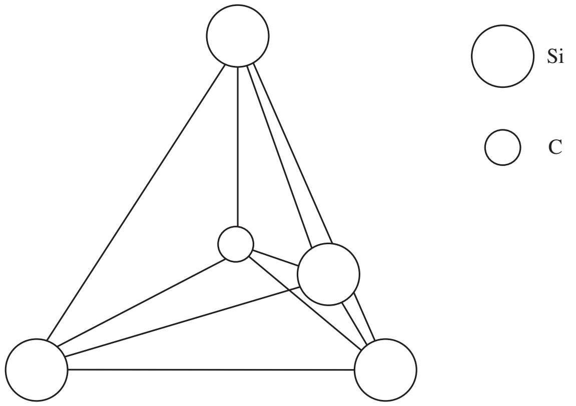

Figure 1. Representation of basic silicon carbide thetraedra.

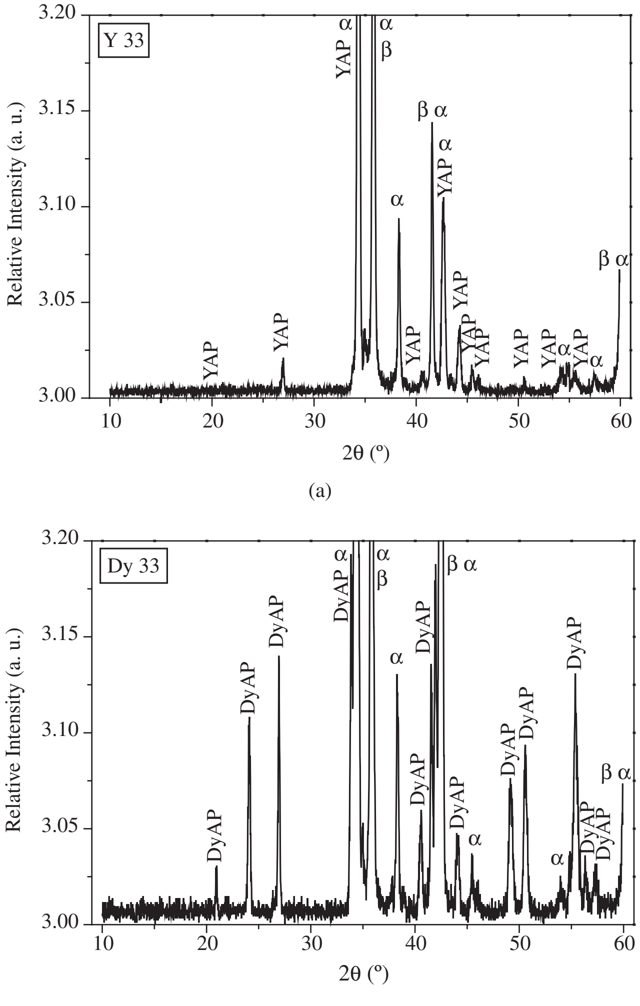

(a)

(b)

Figure 2. X-ray diffratograms patterns of RE 33 samples sintered at 1800 °C/1h: a) RE = Y; b) RE = Dy.

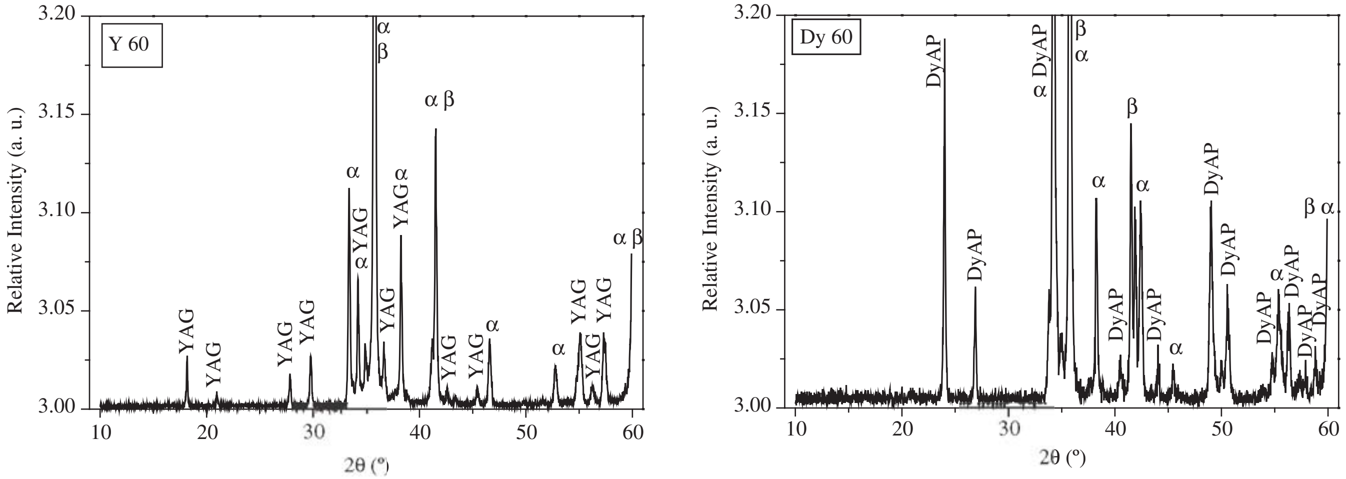

(a) (b)

Figure 3. X-ray diffratograms patterns of RE 60 samples sintered at 1800 °C/1h: a) RE = Y; b) RE = Dy.

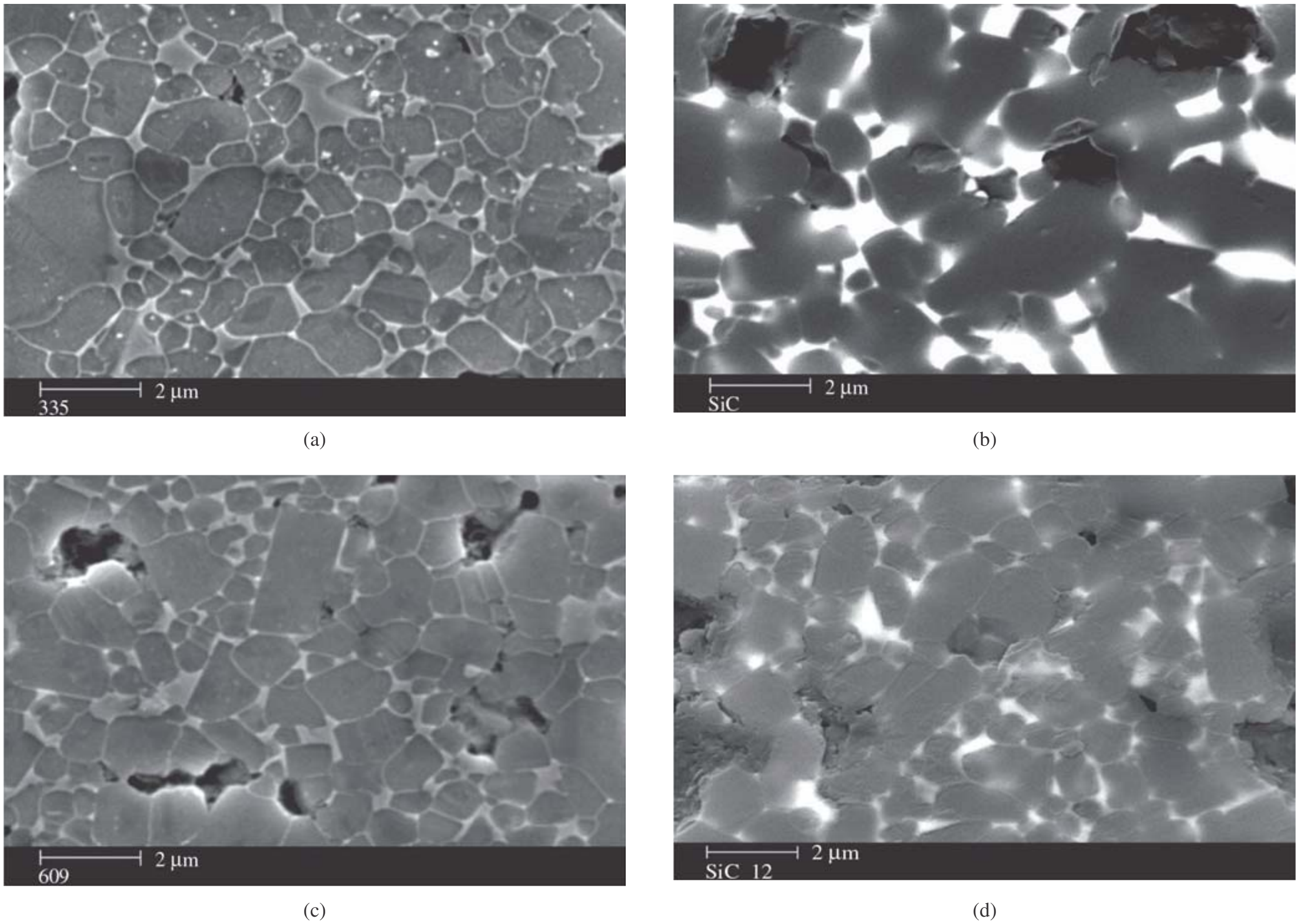

(a) (b) (c) (d)

Figure 4. Scanning electron micrographs of sintered and plasma etched samples: a) Y 33; b) Dy 33; c) Y60; d) Dy 60.

3.3. Dilatometric analysis

Linear shrinkage, determined from dilatometric experiments, of all the samples are show in Figure 5. It can be seen that at dwell temperature (1950 °C) there is no shrinkage, indicating that the densification process of all samples at this temperature is hindered. The sintering behavior of silicon carbide with oxide additives is similar to that of silicon nitride based ceramics.

The density results of samples sintered in the furnace with graphite elements are in good agreement with those obtained from the dilatometric experiments and are shown in Figure 5.

The corresponding linear shrinkage rates are shown in Figure 6. The sintering behavior is clearly dependent on the additive.

The samples with RE33 (RE = Y, Dy) composition (Figure 6a) present three peaks of maximum shrinkage rate (T1, T2, T4) and one peak of minimum shrinkage rate (T3). T1, a low temperature peak, is related to particle rearrangement and the formation of the first liquid. The T2 peak is related to dissolution-re-precipitation of silicon carbide grains, similar to that in silicon nitride ceramics. This process is hindered through out secondary crystalline phase(s) formation (T3 peak). When the temperature is increased, these phases dissolve and the energy is enough to promote dissolution-re-precipitation of silicon carbide grains, indicated by the T4 peak. The temperatures of these peaks are shown in Table 4.

The samples with RE60 (RE = Y, Dy) compositions (Figura 6b) present two peaks of maximum shrinkage rate. The first one, at the lower temperature (at 1310 °C and 1235 °C for samples sintered with yttria and disprosia, respectively) and broader, indicates a slight rearrangement of silicon carbide particles as the liquid phase starts to form, at a temperature near the eutectic. The sharper peak observed at the higher temperature in Figure 6b (1725 °C and 1700 °C for samples sintered with yttria and disprosia, respectively) represents the formation of a larger amount of liquid and simultaneous dissolution of silicon carbide particles, the so called dissolution-re-precipitation process.

The existence of only one peak of maximum shrinkage rate, due to the dissolution-re-precipitation process, in RE60 samples is related to the fact that these samples are located in the glass-forming region, and, consequently, to the absence of secondary crystalline phases, which hinder the dissolution-re-precipitation process.

In the samples with RE60 compositions, the temperature of maximum shrinkage rate, due to the dissolution-re-precipitation process (T4 peak) are lower than that for RE33 samples. The latter samples must overcome the kinetic barrier caused by the formation of secondary crystalline phase. This process requires higher temperatures to promote the dissolution-re-precipitation process at higher rates.

Table 4. Temperatures (°C) of maximum or minumum shrinkage rate for samples sintered in dilatometer at 1950 °C/1h (see text for details).

sample	Samples sintered with yttria				Samples sintered with disprosia			
	T1	T2	T3	T4	T1	T2	T3	T4
RE33	1295	1595	1700	1800	1265	1615	1725	1785

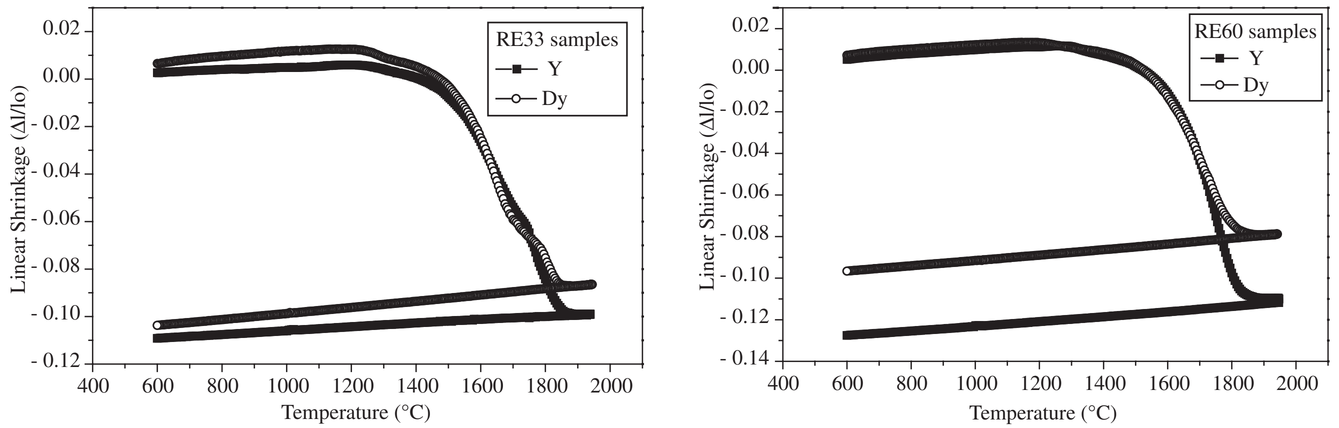

(a) (b)

Figure 5. Dilatometric results: linear shrinkage versus temperature for several compositions: a) RE 33 samples (RE = Y, Dy); b) RE 60 samples (RE = Y, Dy).

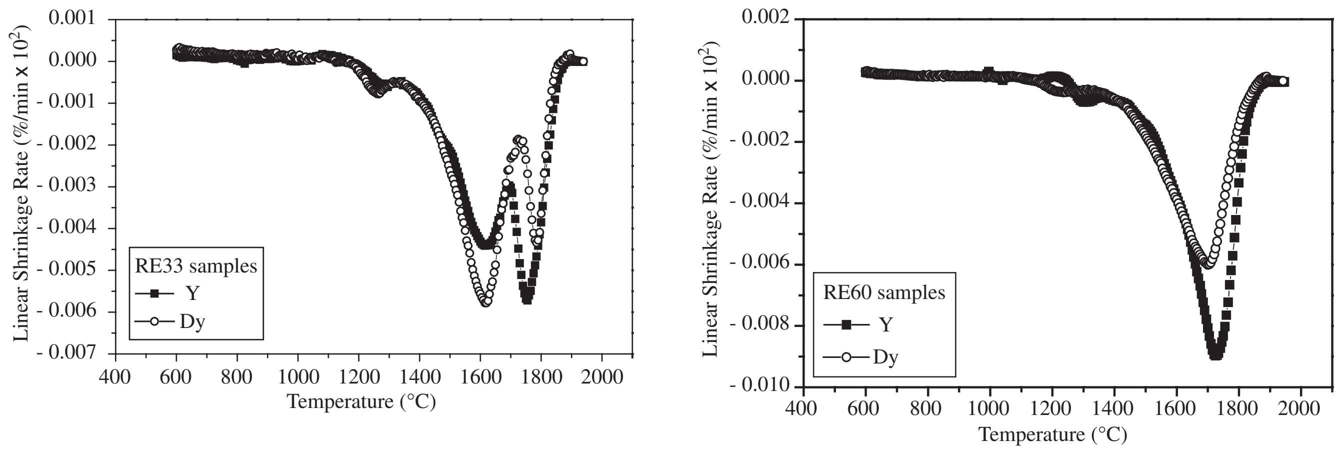

(a) (b)

Figure 6. Dilatometric results: linear shrinkage rate versus temperature for several compositions: a) RE 33 samples (RE = Y, Dy); b) RE 60 samples (RE = Y, Dy).

Moreover, samples sintered with yttria have T4 temperature higher than samples sintered with dysprosia, due probably to the lower viscosity of yttria liquid phase and a different temperature for dissolution of transient secondary phases.

There is a clear correlation between the position of a specific composition with the additive in the ternary equilibrium diagram of SiO_2-Al_2O_3-RE_2O_3 [24] (RE = Y, Dy), and the tendency of the additive to form secondary crystalline phases or glass-phases and the identification of dilatometric shrinkage rate peaks. To understand the sintering kinetics of silicon carbide based materials, X-ray diffraction analysis data was essential as it enabled the identification of secondary crystalline phases formed at specific temperatures. The formation of these phases explained the dilatometric behavior of these samples.

4. Conclusions

The use of 10 vol. % of several combinations of additives based on SiO_2, RE_2O_3 and Al_2O_3 was, in general, suitable to obtain high density silicon carbide ceramics by pressureless sintering. Comparison of density data of samples with the same composition revealed that samples sintered with yttria had higher densities than those sintered with dysprosia.

X-ray diffraction analysis revealed the presence of β-SiC and α-SiC in all samples. Several transient phases, with different stoichiometry, were identified. These were crystalline secondary phases in samples sintered with yttria or dysprosia, depending on the heat treatment temperature. The temperature of the crystalline phase formation/dissolution could be estimated. After sintering at 1950 °C, only $RE_4Al_2O_9$ and $RE_2Al_2O_6$ were identified.

Dilatometric experiments revealed the presence of several shrinkage peaks during sintering of silicon carbide. These peaks can be related to particle rearrangement and, at higher temperatures, to liquid formation and dissolution-re-precipitation. Extra peaks are present if secondary crystalline phases are formed and these in general hinder the densification process. This process however continues when these secondary phases are dissolved.

Acknowledgments

The authors thank CNPq, PRONEX and FAPESP for financial support. The diffraction experiments were done at 'Laboratório de Matérias Primas e Sólidos não Metálicos, Departamento de Engenharia Metalúrgica e de Materiais, Escola Politécnica da Universidade de São Paulo', which we also acknowledge and thank.

References

1. Bocke, W, Landfermann H, Hausner H. Sintering of alpha silicon carbide with additions of aluminium. *Powder Metall. Intern*. 1979; 11:83-85.
2. Cao JJ, Moberlychan WJ, De Jonghe LC. Gilber CJ, Ritchie RO. *In situ* toughened silicon carbide with Al-B-C additions. *J. Am. Ceram. Soc*. 1996; 79:461-469.
3. Negita, K. Effective sintering aids for silicon carbide ceramics: reactivities of silicon carbide with various additives. *J. Am. Ceram. Soc*. 1986; 69:c308-c310.
4. Dijen FKV, Mayer E. Liquid phase sintering of silicon carbide. *J. Euro. Ceram. Soc*. 1996; 16:413-420.
5. Keppeler M, Reichert HG, Broadley JM, Thurn G, Wiedmann I, Aldinger F. High temperature mechanical behavior of liquid phase sintered silicon carbide. *J. Euro. Ceram. Soc*. 1998; 18:521-526.
6. Takajo S, Kausser WA, Petzow G. Analysis of particle growth by coalescence during liquid phase sintering. *Acta Mater*. 1984;32:107-113.
7. Zahn G, Ikuhara Y, Mitomo M, Xie R, Sakuma T, Mukherjee AK, Microstructural analysis of liquid phase sintered β-silicon carbide. *J. Am. Ceram. Soc*. 2002; 84:430-436.
8. Pan Y, Baptista JL. Low-temperature sintering of silicon carbide with Li_2O-Al_2O_3-SiO_2 melts as sintering aids. *J. Euro. Ceram. Soc*. 1996; 16:1221-1230.
9. Izhevsky VA, Genova LA, Bressiani AHA, Bressiani JC. Liquid phase sintered SiC. Processing and transformation controlled microstructure tailoring. *Mater. Res*. 2000; 3:131-138.
10. Lee JK, Tanaka H, Kim H, Kim DJ. Microstructural changes in liquid phase sintered α silicon carbide. *Mater. Letters*. 1996; 29:135-142.
11. Karch K, Bechstedt F, Pavone P, Strauch D, Pressure dependent properties of SiC polytypes. *Phisical Review B*.1996; 53:400-413.
12. Frevel LK, Petersen DR, Saha CK, Polytype distribution in silicon carbide. *J. Mater. Sci*. 1992; 27:1913-1925.
13. Zhou Y, Hirao K, Toriyama M, Kanzaki S, Effects of intergranular phase chemistry on microstructure and mechanical properties of silicon carbide ceramics densified with rare earth oxide and alumina additions. *J. Am. Ceram. Soc*. 2001; 84:1642-1644.
14. Jou ZC, Virkar AV, Cutler RA. High temperature creep of SiC densified using a transient liquid phase. *J. Am. Ceram. Soc*. 1991; 74:1945-1949.
15. Kim Y. High temperature strength of liquid phase sintered SiC with AlN and Re_2O_3 (RE = Y, Yb), *J. Am. Ceram. Soc*. 2002; 85:1007-1009.
16. Izhevskyi VA, Genova LA, Bressiani AHA, Bressiani JC. Liquid phase sintered silicon carbide based ceramics with AlN-Y_2O_3 and AlN-La_2O_3 additives. *Ceramic Materials and Components for Engines*, p. 593-598, Wiley VCH, Weinhein, Ed. J. G Heinrich and F. Aldinger, 2001.
17. Omori M, Takei H. Preparation of pressureless-sintered SiC-Y_2O_3-Al_2O_3. *J. Mater. Sci*. 1988; 23:3744-3749.
18. Mulla MA, Krstic VD. Low temperature pressureless sintering of β-silicon carbide with aluminium oxide and yttrium oxide additions. *Am. Ceram. Soc. Bull*. 1991; 70:439-443.
19. Winn EJ, Clegg WJ, Role of powder bed. I. The densification of silicon carbide sintered with yttria and alumina additives. *J. Am. Ceram. Soc*. 1999; 82:3466-3470.
20. Camusai N, Thompson DP, Mandal H. Effect of starting composition, type of rare earth sintering additive and amount of liquid phase on α–β sialon transformation. *J. Euro. Ceram. Soc*. 1997; 17:599-613.
21. Hirosaki N, Okada A, Matoba K, Sintering of Si_3N_4 with the addition of rare-earth-oxides. *J. Am. Ceram. Soc*. 1988; 71:c144-c147.
22. Huang ZK, Rosenflanz A, Chen IW. Pressureless sintering of Si_3N_4 ceramic using AlN and rare-earth oxides. *J.Am. Ceram. Soc*. 1997; 80:1256-1262.
23. Marchi J, Bressiani JC, Bressiani AHA. Densification Studies of Silicon Carbide-Based Ceramics with Yttria, Silica and Alumina as Sintering Additives. *Mater. Res*. 2001; 4:231-236.
24. Bondar A, Galakhov FY. System Al_2O_3-Y_2O_3-SiO_2. In Levin, E. M., Robbins, C. R., McMurdie, H. F., Phase diagram for Ceramists, Supplement, p. 107, *The American Ceramic Society*, 1969.